Geophys. J. Int. (2009) **178,** 813–825 doi: 10.1111/j.1365-246X.2009.04177.x

Time-frequency misfit and goodness-of-fit criteria for quantitative comparison of time signals

Miriam Kristeková,[1] Jozef Kristek[2] and Peter Moczo[2]

[1]*Geophysical Institute, Slovak Academy of Sciences, Dubravska cesta* 9, 845 28 *Bratislava, Slovak Republic*
[2]*Faculty of Mathematics, Physics and Informatics, Comenius University Bratislava, Mlynska dolina* F1, 842 48 *Bratislava, Slovak Republic.*
E-mail: moczo@fmph.uniba.sk

Accepted 2009 March 10. Received 2009 March 5; in original form 2008 October 10

SUMMARY

We present an extension of the theory of the time-frequency (TF) misfit criteria for quantitative comparison of time signals. We define TF misfit criteria for quantification and characterization of disagreement between two three-component signals. We distinguish two cases—with and without having one signal as reference. We define locally and globally normalized TF criteria.

The locally normalized misfits can be used if it is important to investigate relatively small parts of the signal (e.g. wave groups, pulses, transients, spikes, so-called seismic phases) no matter how large amplitudes of those parts are with respect to the maximum amplitude of the signal. They provide a detailed TF anatomy of the disagreement between two entire signals. The globally normalized misfits can be used for quantifying an overall level of disagreement. They allow accounting for both the envelope/phase difference at a TF point and the significance of the envelope at that point with respect to the maximum envelope of the signal.

We also introduce the TF envelope and phase goodness-of-fit criteria based on the complete signal representation, and thus suitable for comparing arbitrary time signals in their entire TF complexity. The TF goodness-of-fit criteria quantify the level of agreement and are most suitable in the case of larger differences between the signals.

We numerically demonstrate the capability and important features of the TF misfit and goodness-of-fit criteria in the methodologically important examples.

Key word: Time series analysis.

1 INTRODUCTION

Quantitative comparison of time signals, time histories of physical or chemical quantities is often necessary in many problems. Developing and testing a new theoretical method of calculation requires comparison of a theoretical signal with a reference or exact solution. Comparison of a theoretical signal with a measured one is necessary to verify the theoretical model of an investigated process. Comparison of two measured signals significantly helps in the analysis and interpretation of the process under investigation.

A simple visual comparison of two signals can be useful in some cases. Sometimes the simplest possible misfit, a difference $D(t) = s(t) - sr(t)$ between the tested signal $s(t)$ and reference signal $sr(t)$, t being time, is better. A single-valued integral quantity is more appropriate if a set of signals is to be compared with another set of signals. A simple single-valued misfit between two signals can be defined as $MD = \sum_t |D(t)| / \sum_t |sr(t)|$. Probably the root mean square (rms) misfit, $\text{rms} = \sqrt{\sum_t |D(t)|^2 / \sum_t |sr(t)|^2}$ is the most commonly used single-valued misfit criterion.

Although each of the three above quantities somehow estimates a difference between two signals, it is not so difficult to find out that none of them is capable to characterize the nature or reason of the difference. Consequently and eventually it is not clear at all whether they are capable to properly quantify the difference. Therefore, Kristekova *et al.* (2006) developed time-frequency (TF) envelope and phase misfit criteria and demonstrated their capability to properly quantify and characterize a difference between two signals.

The very basic arguments for developing criteria based on the TF representation of signals that are to be compared are:

1. One of the two signals can be viewed as some modification of the other signal. It is clear then that some modifications of the signal can be more visible and understandable in the time domain, some in the frequency domain. Some modifications can change mainly or only amplitudes and an envelope, some other a phase.
2. The most complete and informative characterization of a signal can be obtained by its TF representation (in this sense we can also say decomposition in the TF plane). The TF representation enables us to see a spectral content at any time as well as time history at any frequency.

The TF criteria of Kristekova *et al.* (2006) were applied, for example by Pérez-Ruiz *et al.* (2007), Moczo *et al.* (2007), Benjemaa *et al.* (2007), Käser *et al.* (2008), Fichtner & Igel (2008) and Santoyo & Luzon (2008). The criteria were also used for

evaluation of the international numerical benchmark ESG 2006 for Grenoble valley (Tsuno *et al.* 2006; Chaljub *et al.* 2009a,b), Bielak *et al.* (2008) applied the criteria to compare three numerical simulations for the ShakeOut earthquake scenario version 1.1 for the southern California. The criteria serve for comparison of submitted solutions in the framework of the SPICE Code Validation (Igel *et al.* 2005; Moczo *et al.* 2006; Gallovic *et al.* 2007, http://www.nuquake.eu/SPICECVal/). The recently organized numerical benchmark for the ground motion simulation for the Euroseistest site, Mygdonian basin, Greece (https://www-cashima.cea.fr/) will also apply the TF misfit criteria for evaluation of the submitted predictions.

The paper by Kristekova *et al.* (2006) presented TF misfit criteria for one-component signals in the case when one of the two signals could be considered a reference. The paper emphasized the globally normalized criteria and only marginally mentioned the locally normalized criteria.

Clearly, the paper presented by Kristekova *et al.* (2006) did not address all important aspects and situations in comparing signals in the research practice. This was also clear from frequently asked questions arising in response to the paper. The questions basically concern the following.

(1) The definition of the TF misfits in the case when none of signals can be considered a reference.
(2) The application of the TF misfits to three-component signals.
(3) The applicability of the TF misfits if the signals, that are to be compared, differ 'too much', and consequently the relation of the TF misfit criteria to the goodness-of-fit criteria.
(4) The global versus local normalization.
(5) The evaluation and interpretation of the phase misfits, mainly the relation to the phase jumps.

Correspondingly, in this paper we first briefly summarize the very basic concepts and relations necessary for the further exposition. We then pay attention to the concepts of the envelope and phase differences, and strategies for defining TF misfit criteria. We continue with definitions of the TF misfit criteria for three-component signals in both situations—with and without having a reference signal. Whereas the misfit criteria are supposed to quantify and characterize differences between signals, goodness-of-fit criteria are supposed to quantify the level of agreement between signals. For such situations we introduce TF goodness-of-fit criteria and discuss their relation to the TF misfit criteria. Eventually we numerically illustrate the TF misfit and goodness-of-fit criteria using two methodologically important problems.

2 CHARACTERIZATION OF A SIGNAL

Here we only very briefly present concepts and relations for characterization of a signal necessary in the further exposition.

2.1 Basic characteristics of a simple signal

In the simplest case of a monochromatic signal

$$s_m(t) = A\ \cos(2\pi f t + \phi) \tag{1}$$

amplitude A, phase ϕ and frequency f are unambiguously defined and very easy to interpret. If a signal is more complex, notion of amplitude, phase and frequency may be not so obvious because, for example, when $A = A(t)$, $f = f(t)$ and $\phi = \phi(t)$ in the argument of the cosine function, amplitude and phase are ambiguous.

The analytical signal (e.g. Flandrin 1999) enables us to develop proper unambiguous characteristics. The analytical signal $\tilde{s}(t)$ with respect to signal $s(t)$ is

$$\tilde{s}(t) = s(t) + \mathrm{i}\, H\{s(t)\}, \tag{2}$$

where $H\{s(t)\}$ is the Hilbert transform of signal $s(t)$. Relations

$$A(t) = |\tilde{s}(t)|, \quad \phi(t) = \mathrm{Arg}[\tilde{s}(t)], \tag{3}$$

and

$$f(t) = \frac{1}{2\pi}\frac{\mathrm{d}\,\mathrm{Arg}\,[\tilde{s}(t)]}{\mathrm{d}t}$$

define envelope, phase and (so-called instantaneous) frequency of the signal at time t. Although these quantities are unambiguous, they, in fact, represent just averaged values. For example, Qian (2002) suggests using a term 'the mean instantaneous frequency' instead of the instantaneous frequency. The narrower the spectral content at time t is, the better is the estimate of the dominant amplitude, phase, and frequency by relations (3).

Although the concept of the analytical signal can be applied to simple signals and serve as a basis for simple misfit criteria (e.g. Kristek *et al.* 2002; Kristek & Moczo 2006), it clearly cannot be applied to signals with a complex spectral contents changing with time if the three basic characteristics are to be determined.

2.2 Time-frequency representation of a signal

An instantaneous spectral content of a signal or a time evolution at any frequency of the signal can be obtained using the TF representation of the signal. The TF representation can be obtained using, for example, the continuous wavelet transform. The continuous wavelet transform of signal $s(t)$ is defined by

$$CWT_{(a,b)}\{s(t)\} = \frac{1}{\sqrt{|a|}}\int_{-\infty}^{\infty} s(t)\psi^*\left(\frac{t-b}{a}\right)\mathrm{d}t \tag{4}$$

with t being time, a the scale parameter, b translational parameter, and ψ analysing wavelet. Star denotes the complex conjugate function. The scale parameter a is inversely proportional to frequency f. Consider an analysing wavelet with a spectrum, which has zero amplitudes at negative frequencies. Such a wavelet is an analytical signal and is called the progressive wavelet. A Morlet wavelet

$$\psi(t) = \pi^{-1/4}\exp(\mathrm{i}\omega_0 t)\exp(-t^2/2) \tag{5}$$

with $\omega_0 = 6$ is a proper choice for a wide class of signals and problems. The TF representation of signal $s(t)$ based on the continuous wavelet transform, $W(t, f)$, can be then defined by choosing a relation between the scale parameter a and frequency f in the form $a = \omega_0/.2\,\pi f$, and replacing b by t (because the translational parameter b corresponds to time). We obtain

$$W(t, f) = CWT_{(f,t)}\{s(t)\} = \sqrt{\frac{2\pi|f|}{\omega_0}}\int_{-\infty}^{\infty} s(\tau)\psi^*\left(2\pi f\frac{\tau - t}{\omega_0}\right)\mathrm{d}\tau. \tag{6}$$

$W^2(t, f)$ represents the energy distribution (energy density) of the signal in the TF plane. A more detailed mathematical background on the continuous wavelet transform and Morlet wavelet can be found, for example, in monographs by Daubechies (1992) and Holschneider (1995), Kristekova *et al.* (2006, 2008b) numerically demonstrated very good properties of the TF representation defined above.

Having determined the TF representation, an envelope $A(t, f)$ and phase $\phi(t, f)$ at a given point of the TF plane can be defined

$$A(t, f) = |W(t, f)|, \quad \phi(t, f) = \mathrm{Arg}[W(t, f)]. \tag{7}$$

Holschneider (1995) showed that if $W(t, f)$ is defined using the continuous wavelet transform with the progressive wavelet, the envelope $A(t, f)$ and phase $\phi(t, f)$ are consistent with those defined using the analytical signal.

Note that this TF representation does not suffer from the well-known problems and limitations of the windowed Fourier transform due to the fixed TF resolution of the windowed Fourier transform.

The software package SEIS-TFA developed by Kristekova (2006) for numerical computation of the TF representation using the continuous wavelet transform and six other methods is available at http://www.nuquake.eu.

3 COMPARISON OF SIGNALS

3.1 TF envelope and phase differences

Consider a signal $s(t)$ and a reference signal $sr(t)$. Given (6) and (7) it is clear that

$$\Delta A(t, f) = A(t, f) - Ar(t, f) = |W(t, f)| - |Wr(t, f)| \tag{8}$$

defines the difference between two envelopes at each (t, f) point. Similarly,

$$\begin{aligned}\Delta\phi(t, f) &= \phi(t, f) - \phi r(t, f) \\ &= \mathrm{Arg}[W(t, f)] - \mathrm{Arg}[Wr(t, f)]\end{aligned} \tag{9}$$

defines the difference between two phases at each (t, f) point.

The envelope difference $\Delta A(t, f)$ is an absolute local difference that can attain any value. The phase difference needs some explanation. The little complication comes from the fact that Arg $[\xi]$ always gives the phase of the complex variable ξ in the range of $\langle -\pi, \pi \rangle$. If, for example, two phases are $170\pi/180$ and $-160\pi/180$, eq. (9) formally gives $330\pi/180$ instead of the correct value $-30\pi/180$. It is clear that definition (9) would need an additional condition to treat similar situations. Instead, however, we can avoid this complication using the following equivalent definition

$$\Delta\phi(t, f) = \mathrm{Arg}\left[\frac{W(t, f)}{Wr(t, f)}\right]. \tag{10}$$

Relation (10) always gives a local phase difference in the range of $\langle -\pi, \pi \rangle$.

3.2 Strategies for defining TF misfit criteria

Having the envelope and phase differences at a given (t, f) point, we can define a variety of the TF misfit criteria to quantitatively compare the entire signals, important parts or characteristics of the signals.

In many problems it is important to investigate relatively small parts of the signal (e.g. wave groups, pulses, transients, spikes, so-called seismic phases) no matter how large amplitudes of those parts are with respect to the maximum amplitude of the entire signal. As an example of an important seismic phase we can mention the mantle phase *PcP*—the seismic *P* wave reflected at the core–mantle boundary. In some problems one may be interested in a detailed TF anatomy of the disagreement between two entire signals. For comparing two signals in such situations we need to define local misfit criteria–criteria whose values for one (t, f) point would depend only on the characteristics at that (t, f) point. Consider a local TF misfit criterion for the envelope. It is clear that such criterion should quantify the relative difference between two envelopes at a given (t, f) point. Consequently, $\Delta A(t, f)$ given by eq. (8) should be normalized by $Ar(t, f)$. At the same time, due to its nature, the phase difference (10) itself provides the proper quantification for a local TF phase misfit criterion. We can choose, however, the range $\langle -1, 1 \rangle$ instead of $\langle -\pi, \pi \rangle$: we can divide the phase difference (10) by π.

The preceding considerations can be taken as arguments and basis for defining the locally normalized TF misfit criteria. Then

$$TFEM_{\mathrm{LOC}}(t, f) = \frac{\Delta A(t, f)}{Ar(t, f)} \tag{11}$$

and

$$TFPM_{\mathrm{LOC}}(t, f) = \frac{\Delta\phi(t, f)}{\pi} \tag{12}$$

define the locally normalized TF envelope ($TFEM_{\mathrm{LOC}}$) and phase ($TFPM_{\mathrm{LOC}}$) misfit criteria, respectively.

In some analyses it may be reasonable to give the largest weights to local envelope/phase differences for those parts of the reference signal in which the envelope reaches the largest values. For example, it may be reasonable to require that the envelope misfit be equal to the absolute local envelope difference $\Delta A(t, f)$ just at that (t, f) point at which envelope $Ar(t, f)$ of the reference signal reaches its maximum $\max_{t,f}\{Ar(t, f)\}$. At the other (t, f) points with the envelope smaller than $\max_{t,f}\{Ar(t, f)\}$ (and therefore also with smaller energy content) such a misfit could be proportional to the ratio between $Ar(t, f)$ and $\max_{t,f}\{Ar(t, f)\}$. Both requirements are met in the following definitions

$$\begin{aligned}TFEM_{\mathrm{GLOB}}(t, f) &= \frac{Ar(t, f)}{\max_{t,f}\{Ar(t, f)\}} TFEM_{\mathrm{LOC}}(t, f) \\ &= \frac{\Delta A(t, f)}{\max_{t,f}\{Ar(t, f)\}},\end{aligned} \tag{13}$$

$$\begin{aligned}TFPM_{\mathrm{GLOB}}(t, f) &= \frac{Ar(t, f)}{\max_{t,f}\{Ar(t, f)\}} TFPM_{\mathrm{LOC}}(t, f) \\ &= \frac{Ar(t, f)}{\max_{t,f}\{Ar(t, f)\}} \frac{\Delta\phi(t, f)}{\pi}.\end{aligned} \tag{14}$$

Because the definitions apply the normalization by $\max_{t,f}\{Ar(t, f)\}$ at each (t, f) point, we can speak of the globally normalized TF envelope ($TFEM_{\mathrm{GLOB}}$) and phase ($TFPM_{\mathrm{GLOB}}$) misfit criteria. Clearly, the values of the globally normalized TF misfit criteria account for both the envelope/phase difference at a (t, f) point and the significance of the envelope at that point with respect to the maximum envelope of the reference signal. In this sense they quantify an overall level of disagreement between two signals. We apply the global normalization in definition of the TF misfits when we are not much interested in a detailed anatomy of the signals and misfits in those parts of the signal where its amplitudes are too small compared to the maximum amplitude of the reference signal. The globally normalized misfit criteria can be useful, for example, in the earthquake ground motion analyses and earthquake engineering where we are usually not much interested in particular wave groups with relatively small amplitudes.

4 TF MISFIT CRITERIA FOR THREE-COMPONENT SIGNALS

4.1 Three-component signals, one signal being a reference

The above considerations on the globally normalized misfit criteria for one-component signals can be extended also to the misfits for three-component signals. If amplitudes of one component of the reference signal are significantly smaller than amplitudes of two other components (a common situation with a polarized particle motion, for example), the only reasonable choice for the global normalization is to take the maximum TF envelope value from all three components of the reference signal. This choice naturally quantifies the misfits with respect to the meaningful values of the three-component reference signal. It also prevents obtaining too large misfit values due to possible division by very small envelope values corresponding to insignificant amplitudes of the signal components. Clearly, this choice is reasonable also if the amplitudes of all three components of the signals are comparable.

A formal definition of one local normalization factor for all three components would clearly contradict to the local character. Each component has to be treated as, one-component" signal if one is interested in the detailed anatomy of the TF misfit.

Now we can define a set of the misfit criteria for the three-component signals when one of them can be considered a reference. The locally normalized and globally normalized TF envelope misfits $TFEM^{\mathrm{REF}}_{\mathrm{LOC},i}(t,f)$ and $TFEM^{\mathrm{REF}}_{\mathrm{GLOB},i}(t,f)$, and locally normalized and globally normalized TF phase misfits $TFPM^{\mathrm{REF}}_{\mathrm{LOC},i}(t,f)$ and $TFPM^{\mathrm{REF}}_{\mathrm{GLOB},i}(t,f)$ characterize how the envelopes and phases of the two signals differ at each (t,f) point. Their projection onto the time domain gives time-dependent envelope and phase misfits, $TEM^{\mathrm{REF}}_{\mathrm{LOC},i}(t)$, $TEM^{\mathrm{REF}}_{\mathrm{GLOB},i}(t)$, $TPM^{\mathrm{REF}}_{\mathrm{LOC},i}(t)$ and $TPM^{\mathrm{REF}}_{\mathrm{GLOB},i}(t)$. Similarly, the projection of the TF misfits onto the frequency domain gives frequency-dependent envelope and phase misfits, $FEM^{\mathrm{REF}}_{\mathrm{LOC},i}(f)$, $FEM^{\mathrm{REF}}_{\mathrm{GLOB},i}(f)$, $FPM^{\mathrm{REF}}_{\mathrm{LOC},i}(f)$ and $FPM^{\mathrm{REF}}_{\mathrm{GLOB},i}(f)$. Finally, it is often very useful to have single-valued envelope and phase misfits, $EM^{\mathrm{REF}}_{\mathrm{LOC},i}$, $EM^{\mathrm{REF}}_{\mathrm{GLOB},i}$, $PM^{\mathrm{REF}}_{\mathrm{LOC},i}$ and $PM^{\mathrm{REF}}_{\mathrm{GLOB},i}$. All the misfits are summarized in Tables 1 and 2. The envelope and phase misfits can attain any value in the range $\langle -\infty, \infty\rangle$ and $\langle -1, 1\rangle$, respectively.

4.2 Three-component signals, none being a reference

The misfit criteria for this case can be defined, in fact, formally in the same way as criteria in the case with a reference signal. The only question is which of the two signals should be formally taken as a reference. The reasonable way is to find a maximum envelope for each of the two signals. Then the signal with a smaller maximum can be chosen as a reference signal. In the case of the globally normalized criteria for the three-component signals the maximum

Table 1. Locally and globally normalized TF misfit criteria for three-component signals, one signal being a reference.

$s_i(t)\,; i=1,2,3$	A three-component signal
$sr_i(t)\,;\ i=1,2,3$	A three-component reference signal
$W_i = W_i(t,f)$	*TF* representation of signal $s_i(t)$
$Wr_i = Wr_i(t,f)$	*TF* representation of the reference signal $sr_i(t)$

Time-frequency envelope and phase misfits

Locally normalized TF envelope misfit

$$TFEM^{\mathrm{REF}}_{\mathrm{LOC},i}(t,f) = \frac{|W_i| - |Wr_i|}{|Wr_i|}$$

Locally normalized TF phase misfit

$$TFPM^{\mathrm{REF}}_{\mathrm{LOC},i}(t,f) = \frac{1}{\pi}\mathrm{Arg}\left[\frac{W_i}{Wr_i}\right]$$

Globally normalized TF $\left\{\begin{matrix}\text{envelope}\\ \text{phase}\end{matrix}\right\}$ misfit

$$\begin{Bmatrix} TFEM^{\mathrm{REF}}_{\mathrm{GLOB},i}(t,f) \\ TFPM^{\mathrm{REF}}_{\mathrm{GLOB},i}(t,f) \end{Bmatrix} = \frac{|Wr_i|}{\max_{i;\,t,f}(|Wr_i|)} \begin{Bmatrix} TFEM^{\mathrm{REF}}_{\mathrm{LOC},i}(t,f) \\ TFPM^{\mathrm{REF}}_{\mathrm{LOC},i}(t,f) \end{Bmatrix}$$

Time-dependent envelope and phase misfits

Locally normalized

$$\begin{Bmatrix} TEM^{\mathrm{REF}}_{\mathrm{LOC},i}(t) \\ TPM^{\mathrm{REF}}_{\mathrm{LOC},i}(t) \end{Bmatrix} = \frac{\sum_f |Wr_i| \begin{Bmatrix} TFEM^{\mathrm{REF}}_{\mathrm{LOC},i}(t,f) \\ TFPM^{\mathrm{REF}}_{\mathrm{LOC},i}(t,f) \end{Bmatrix}}{\sum_f |Wr_i|}$$

Globally normalized

$$\begin{Bmatrix} TEM^{\mathrm{REF}}_{\mathrm{GLOB},i}(t) \\ TPM^{\mathrm{REF}}_{\mathrm{GLOB},i}(t) \end{Bmatrix} = \frac{\sum_f |Wr_i| \begin{Bmatrix} TFEM^{\mathrm{REF}}_{\mathrm{LOC},i}(t,f) \\ TFPM^{\mathrm{REF}}_{\mathrm{LOC},i}(t,f) \end{Bmatrix}}{\max_{i;\,t}\left(\sum_f |Wr_i|\right)}$$

Frequency-dependent envelope and phase misfits

Locally normalized

$$\begin{Bmatrix} FEM^{\mathrm{REF}}_{\mathrm{LOC},i}(f) \\ FPM^{\mathrm{REF}}_{\mathrm{LOC},i}(f) \end{Bmatrix} = \frac{\sum_t |Wr_i| \begin{Bmatrix} TFEM^{\mathrm{REF}}_{\mathrm{LOC},i}(t,f) \\ TFPM^{\mathrm{REF}}_{\mathrm{LOC},i}(t,f) \end{Bmatrix}}{\sum_t |Wr_i|}$$

Globally normalized

$$\begin{Bmatrix} FEM^{\mathrm{REF}}_{\mathrm{GLOB},i}(f) \\ FPM^{\mathrm{REF}}_{\mathrm{GLOB},i}(f) \end{Bmatrix} = \frac{\sum_t |Wr_i| \begin{Bmatrix} TFEM^{\mathrm{REF}}_{\mathrm{LOC},i}(t,f) \\ TFPM^{\mathrm{REF}}_{\mathrm{LOC},i}(t,f) \end{Bmatrix}}{\max_{i;\,f}\left(\sum_t |Wr_i|\right)}$$

Single-valued envelope and phase misfits

Locally normalized

$$\begin{Bmatrix} EM^{\mathrm{REF}}_{\mathrm{LOC},i} \\ PM^{\mathrm{REF}}_{\mathrm{LOC},i} \end{Bmatrix} = \sqrt{\frac{\sum_f \sum_t |Wr_i|^2 \left| \begin{Bmatrix} TFEM^{\mathrm{REF}}_{\mathrm{LOC},i}(t,f) \\ TFPM^{\mathrm{REF}}_{\mathrm{LOC},i}(t,f) \end{Bmatrix} \right|^2}{\sum_f \sum_t |Wr_i|^2}}$$

Globally normalized

$$\begin{Bmatrix} EM^{\mathrm{REF}}_{\mathrm{GLOB},i} \\ PM^{\mathrm{REF}}_{\mathrm{GLOB},i} \end{Bmatrix} = \sqrt{\frac{\sum_f \sum_t |Wr_i|^2 \left| \begin{Bmatrix} TFEM^{\mathrm{REF}}_{\mathrm{LOC},i}(t,f) \\ TFPM^{\mathrm{REF}}_{\mathrm{LOC},i}(t,f) \end{Bmatrix} \right|^2}{\max_i\left(\sum_f \sum_t |Wr_i|^2\right)}}$$

Table 2. Locally and globally normalized TF misfit criteria for three-component signals, none being a reference.

$s1_i(t),\ \ s2_i(t)\ ;\ i = 1, 2, 3$ — two 3-component signals

$W1_i = W1_i(t, f)\ ,\ \ W2_i = W2_i(t, f)$ — *TF* representations of signals $s1_i(t)$ and $s2_i(t)$

$$Wr_i = W1_i \quad \text{if} \quad \max_{i;\,t,f}(|W1_i|) < \max_{i;\,t,f}(|W2_i|)$$
$$= W2_i \quad \text{if} \quad \max_{i;\,t,f}(|W1_i|) \geq \max_{i;\,t,f}(|W2_i|)$$

Time-frequency envelope and phase misfits

Locally normalized TF envelope misfit

$$TFEM_{\mathrm{LOC},i}(t, f) = \frac{|W1_i| - |W2_i|}{|Wr_i|}$$

Locally normalized TF phase misfit

$$TFPM_{\mathrm{LOC},i}(t, f) = \frac{1}{\pi}\mathrm{Arg}\left[\frac{W1_i}{W2_i}\right]$$

Globally normalized TF $\left\{\begin{matrix}\text{envelope}\\ \text{phase}\end{matrix}\right\}$ misfit

$$\begin{Bmatrix} TFEM_{\mathrm{GLOB},i}(t, f) \\ TFPM_{\mathrm{GLOB},i}(t, f) \end{Bmatrix} = \frac{|Wr_i|}{\max_{i;\,t,f}(|Wr_i|)} \begin{Bmatrix} TFEM_{\mathrm{LOC},i}(t, f) \\ TFPM_{\mathrm{LOC},i}(t, f) \end{Bmatrix}$$

Time-dependent envelope and phase misfits

Locally normalized

$$\begin{Bmatrix} TEM_{\mathrm{LOC},i}(t) \\ TPM_{\mathrm{LOC},i}(t) \end{Bmatrix} = \frac{\sum_f |Wr_i| \begin{Bmatrix} TFEM_{\mathrm{LOC},i}(t, f) \\ TFPM_{\mathrm{LOC},i}(t, f) \end{Bmatrix}}{\sum_f |Wr_i|}$$

Globally normalized

$$\begin{Bmatrix} TEM_{\mathrm{GLOB},i}(t) \\ TPM_{\mathrm{GLOB},i}(t) \end{Bmatrix} = \frac{\sum_f |Wr_i| \begin{Bmatrix} TFEM_{\mathrm{LOC},i}(t, f) \\ TFPM_{\mathrm{LOC},i}(t, f) \end{Bmatrix}}{\max_{i;\,t}\left(\sum_f |Wr_i|\right)}$$

Frequency-dependent envelope and phase misfits

Locally normalized

$$\begin{Bmatrix} FEM_{\mathrm{LOC},i}(f) \\ FPM_{\mathrm{LOC},i}(f) \end{Bmatrix} = \frac{\sum_t |Wr_i| \begin{Bmatrix} TFEM_{\mathrm{LOC},i}(t, f) \\ TFPM_{\mathrm{LOC},i}(t, f) \end{Bmatrix}}{\sum_t |Wr_i|}$$

Globally normalized

$$\begin{Bmatrix} FEM_{\mathrm{GLOB},i}(f) \\ FPM_{\mathrm{GLOB},i}(f) \end{Bmatrix} = \frac{\sum_t |Wr_i| \begin{Bmatrix} TFEM_{\mathrm{LOC},i}(t, f) \\ TFPM_{\mathrm{LOC},i}(t, f) \end{Bmatrix}}{\max_{i;\,f}\left(\sum_t |Wr_i|\right)}$$

Single-valued envelope and phase misfits

Locally normalized

$$\begin{Bmatrix} EM_{\mathrm{LOC},i} \\ PM_{\mathrm{LOC},i} \end{Bmatrix} = \sqrt{\frac{\sum_f \sum_t |Wr_i|^2 \left|\begin{Bmatrix} TFEM_{\mathrm{LOC},i}(t, f) \\ TFPM_{\mathrm{LOC},i}(t, f) \end{Bmatrix}\right|^2}{\sum_f \sum_t |Wr_i|^2}}$$

Globally normalized

$$\begin{Bmatrix} EM_{\mathrm{GLOB},i} \\ PM_{\mathrm{GLOB},i} \end{Bmatrix} = \sqrt{\frac{\sum_f \sum_t |Wr_i|^2 \left|\begin{Bmatrix} TFEM_{\mathrm{LOC},i}(t, f) \\ TFPM_{\mathrm{LOC},i}(t, f) \end{Bmatrix}\right|^2}{\max_i\left(\sum_f \sum_t |Wr_i|^2\right)}}$$

is taken from all components. In the case of the locally normalized criteria the reference signal should be chosen separately for each component.

Note that the evaluation of the TF misfits themselves does not give a reason to prefer the smaller of the two maxima. Our choice comes from the possible link to the goodness-of-fit criteria developed by Anderson (2004). We take the smaller maximum consistently with the Anderson's criteria discussed later.

5 TF GOODNESS-OF-FIT CRITERIA

The envelope TF misfits, as defined in the previous chapter, quantify and characterize how much two envelopes differ from each other. Correspondingly, the envelope misfit can attain any value within the range of $(-\infty, \infty)$ with 0 meaning the agreement. While formally applicable to any level of disagreement, clearly, the envelope misfits are most useful for comparing relatively close envelopes.

However, in practice it is often necessary to compare signals whose envelopes differ relatively considerably. Comparison of real records with synthetics in some problems can be a good example. In such a case it is reasonable to look for the level of agreement rather than details of disagreement. The goodness-of-fit criteria provide a suitable tool for this.

The goodness-of-fit criteria approach zero value with an increasing level of disagreement. On the other hand, some finite value is chosen to quantify the agreement.

The TF envelope goodness-of-fit criteria can be introduced on the basis of the TF envelope misfits

$$\begin{aligned} TFEG(t, f) &= A \exp\left\{-|TFEM(t, f)|^k\right\}, \\ TEG(t) &= A \exp\left\{-|TEM(t)|^k\right\}, \\ FEG(f) &= A \exp\left\{-|FEM(f)|^k\right\}, \\ EG &= A \exp\left\{-|EM|^k\right\}, \\ & A > 0, \quad k > 0\ . \end{aligned} \tag{15}$$

Here, factor A quantifies the agreement between two envelopes in terms of the chosen envelope misfit: The envelope goodness-of-fit criterion is equal to A if the envelope misfit is equal to 0. Choice of the exponent k determines sensitivity of the goodness-of-fit value with respect to the misfit value. If $A = 10$ and $k = 1$, the right-hand side of eq. (15) becomes formally similar to Anderson's formula.

Similarly we can define TF phase goodness-of-fit criteria as the goodness-of-fit equivalents to the TF phase misfit criteria:

$$\begin{aligned} TFPG(t, f) &= A\left(1 - |TFPM(t, f)|^k\right) \\ TPG(t) &= A\left(1 - |TPM(t)|^k\right), \\ FPG(f) &= A\left(1 - |FPM(f)|^k\right), \\ PG &= A\left(1 - |PM|^k\right). \end{aligned} \tag{16}$$

Fig. 1 shows the discrete goodness-of-fit values against the misfit values for $A = 10$ and $k = 1$ what we consider a practically

Misfit Envelope	**Misfit** Phase	**Goodness-of-Fit** Numerical value	Verbal value
± 0.00	± 0.0	10	
± 0.11	± 0.1	9	excellent
± 0.22	± 0.2	8	
± 0.36	± 0.3	7	good
± 0.51	± 0.4	6	
± 0.69	± 0.5	5	fair
± 0.92	± 0.6	4	
± 1.20	± 0.7	3	poor
± 1.61	± 0.8	2	
± 2.30	± 0.9	1	
± ∞	± 1.0	0	

Figure 1. Discrete goodness-of-fit values against the misfit values.

reasonable choice for a wide class of problems. Fig. 1 also includes an example of a possible verbal evaluation of fit. The fourth column of the table assigns four verbal degrees or levels to the goodness-of-fit numerical values. This example of the relatively robust verbal evaluation is taken from the paper of Anderson (2004).

Anderson's goodness-of-fit criteria are based on characteristics relevant in the earthquake-engineering applications. He split the investigated frequency range into relatively narrow frequency subintervals. Then he compared seismograms that had been narrow-band-pass filtered for a given subinterval. He evaluated goodness-of-fit criteria defined for the peak acceleration, peak velocity, peak displacement, Arias intensity, the integral of velocity squared, Fourier spectrum and acceleration response spectrum on a frequency-by-frequency basis, the shape of the normalized integrals of acceleration and velocity squared, and the cross correlation. Each characteristic was compared on a scale from 0 to 10, with 10 meaning agreement. Scores for each parameter were averaged to yield an overall quality of fit. Based on the systematic comparison of the horizontal components of recorded earthquake motions Anderson (2004) introduced the following verbal scale for goodness-of-fit: A score below 4 is a poor fit, a score of 4–6 is a fair fit, a score of 6–8 is a good fit, and a score over 8 is an excellent fit.

We think that the example of the TF misfits, TF goodness-of-fits and verbal levels given in Fig. 1 can be reasonably applied to an analysis of earthquake records and simulations and possibly also to some other problems.

We should stress, however, that the choice of the mapping between the TF misfits and TF goodness-of-fits (in our case the choice of the range of the goodness-of-fit criteria $\langle 0,\ A\rangle$ and exponent k), and the choice of the verbal classification should be adjusted to the problem under investigation and should be based on the numerical experience. In other words, the choice should reflect a relevant aspect of the comparative analysis or the capability of a particular theory to model a real process.

We think that the concept of the TF misfits makes it possible to define proper goodness-of-fits and eventually also the verbal classification for the final/overall robust evaluation/comparison of signals.

6 NUMERICAL EXAMPLES

Kristekova *et al.* (2006) showed detailed numerical examples of the TF misfits for signals that were relatively close. The choice of the close signals allowed demonstrating the capability of the TF misfits not only to quantify differences between the signals but also to characterize the origin or nature of the differences (e.g. pure amplitude modification, pure phase modification, translation in time, frequency shift).

Here we focus on very different situations. In the first example, we compare composed dispersive signals. In the second example, we compare signals, which differ considerably—a recorded signal with a synthetic (numerically modelled) signal.

6.1 Dispersive signals

Dispersive signals are important and common because they are due to the wave interference. Dispersive signals provide a good opportunity to illustrate interesting features of the TF phase misfit.

Consider an example of a simple dispersive signal, $u_0(x,t)$,

$$u_0(x,t) = \int_{2\pi/50}^{2\pi/5} \cos\left[\omega t - \frac{\omega x}{c_0(\omega)}\right] d\omega; \quad c_0(\omega) = 4 - \omega - \omega^2. \tag{17}$$

Here, x is a spatial coordinate, t is time. A slight modification of the frequency dependence of the phase velocity in the signal (17) gives a modified signal $u_{0m}(x,t)$,

$$u_{0m}(x,t) = \int_{2\pi/50}^{2\pi/5} \cos\left[\omega t - \frac{\omega x}{c_{0m}(\omega)}\right] d\omega;$$
$$c_{0m}(\omega) = 3.91 - 0.87\omega - 0.8\omega^2. \tag{18}$$

Both signals for $x = 1500$ km are shown in Fig. 2 (top panel), $u_0(x,t)$ in red, $u_{0m}(x,t)$ in black. Consider also a dispersive signal $u_1(x,t)$,

$$u_1(x,t) = 0.8 \int_{2\pi/15}^{2\pi/3} \cos\left[\omega t - \tfrac{\omega x}{c_1(\omega)}\right] \mathrm{d}\omega;$$
$$c_1(\omega) = 5.5 - 0.7\omega - 0.3\omega^2, \tag{19}$$

that could be considered as the first higher mode to $u_0(x,t)$ and $u_{0m}(x,t)$; in this sense and for the purpose of further analysis let us called $u_0(x,t)$ and $u_{0m}(x,t)$ fundamental modes, and $u_1(x,t)$ the first higher mode. The signal for $x = 1500$ km is shown in Fig. 2 (middle panel), in blue.

We can now define two composed dispersive signals

$$ur(t) = u_0(1500,t) + u_1(1500,t),$$
$$u(t) = u_{0m}(1500,t) + u_1(1500,t). \tag{20}$$

Both signals are superpositions of the fundamental mode and first higher mode. The signals differ in the fundamental mode but they share the same first higher mode. The signals are shown in Fig. 2 (bottom panel)—$ur(t)$ in red, $u(t)$ in black. The TF representations of the both composed signals are shown in Fig. 3. It is obvious from the TF representations that each of the two signals comprises two modes. It is also obvious that these two modes cannot be separated (without knowing their definition formulas) only in the time domain or only in the frequency domain because the modes overlap in both domains. The TF representation is necessary to recognize the structure of each of the composed signals.

The TF representations themselves, however, are not enough for comparing the two composed signals. A simple visual comparison of the TF representations of $ur(t)$ and $u(t)$ only partly allows us to recognize but does not allow us to quantify differences between

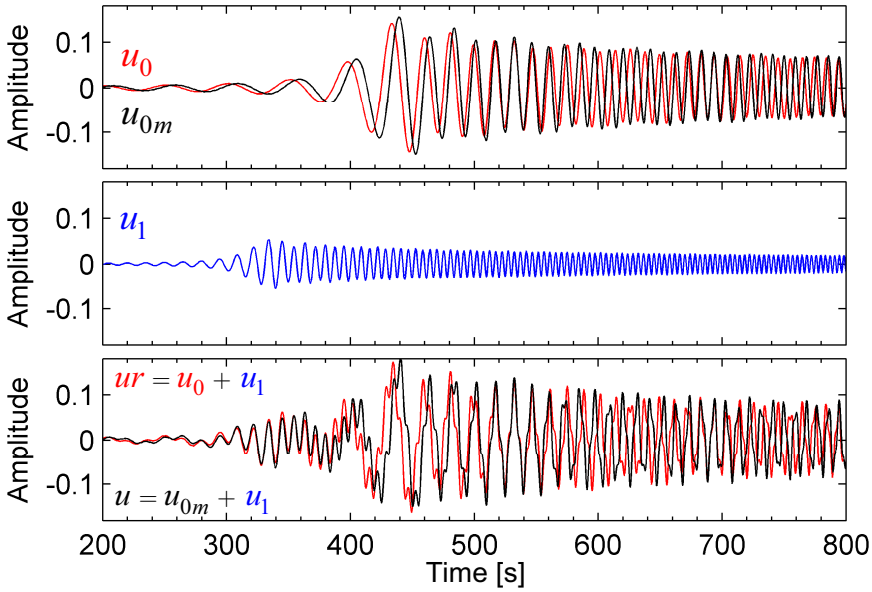

Figure 2. Top panel: dispersive signals $u_0(x, t)$, in red, and $u_{0m}(x, t)$, in black. Middle panel: dispersive signal $u_1(x, t)$ considered as the first higher mode with respect to signals u_0 and u_{0m}. Bottom panel: composed dispersive signals $ur(x, t) = u_0(x, t) + u_1(x, t)$, in red, and $u(x, t) = u_{0m}(x, t) + u_1(x, t)$, in black. All signals are displayed for $x = 1500$.

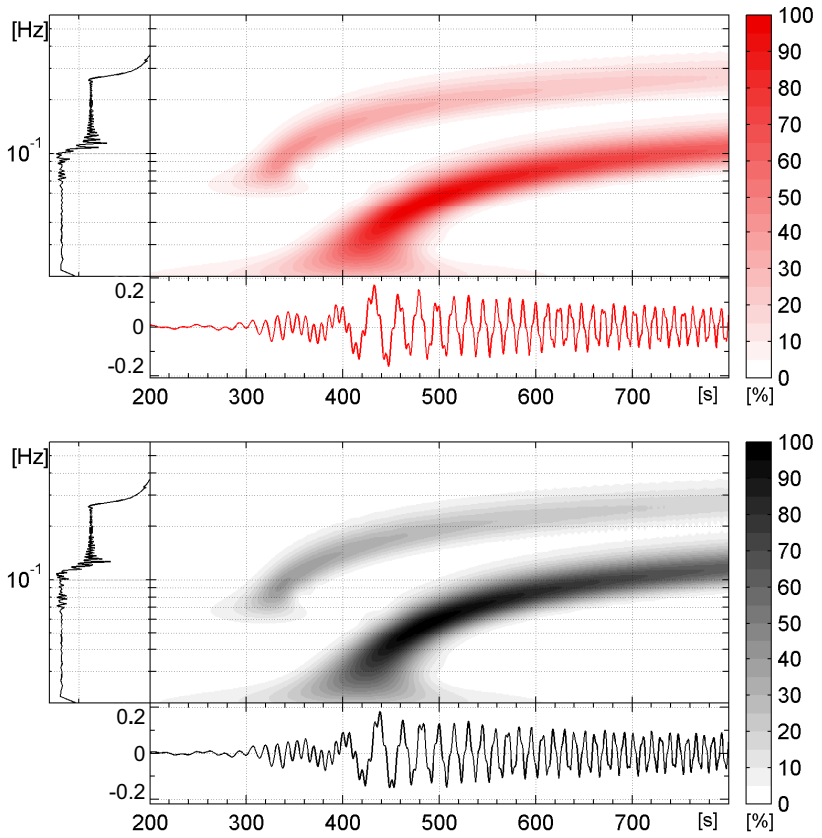

Figure 3. TF representations of the composed dispersive signals $ur(x, t) = u_0(x, t) + u_1(x, t)$, in red, and $u(x, t) = u_{0m}(x, t) + u_1(x, t)$, in black. The signals are displayed for $x = 1500$.

the signals. The TF misfit criteria provide a reasonable tool for the quantitative comparison. The globally normalized TF misfits are displayed in Fig. 4. Both the TF envelope and phase misfits clearly show that $ur(t)$ and $u(t)$ differ only in the fundamental modes—there is no misfit in the TF region corresponding to the first higher mode $u_1(t)$.

TF envelope misfit $TFEM^{\mathrm{REF}}_{\mathrm{GLOB}}(t, f)$ and both the time- and frequency-dependent envelope misfits $TEM^{\mathrm{REF}}_{\mathrm{GLOB}}(t)$ and $FEM^{\mathrm{REF}}_{\mathrm{GLOB}}$

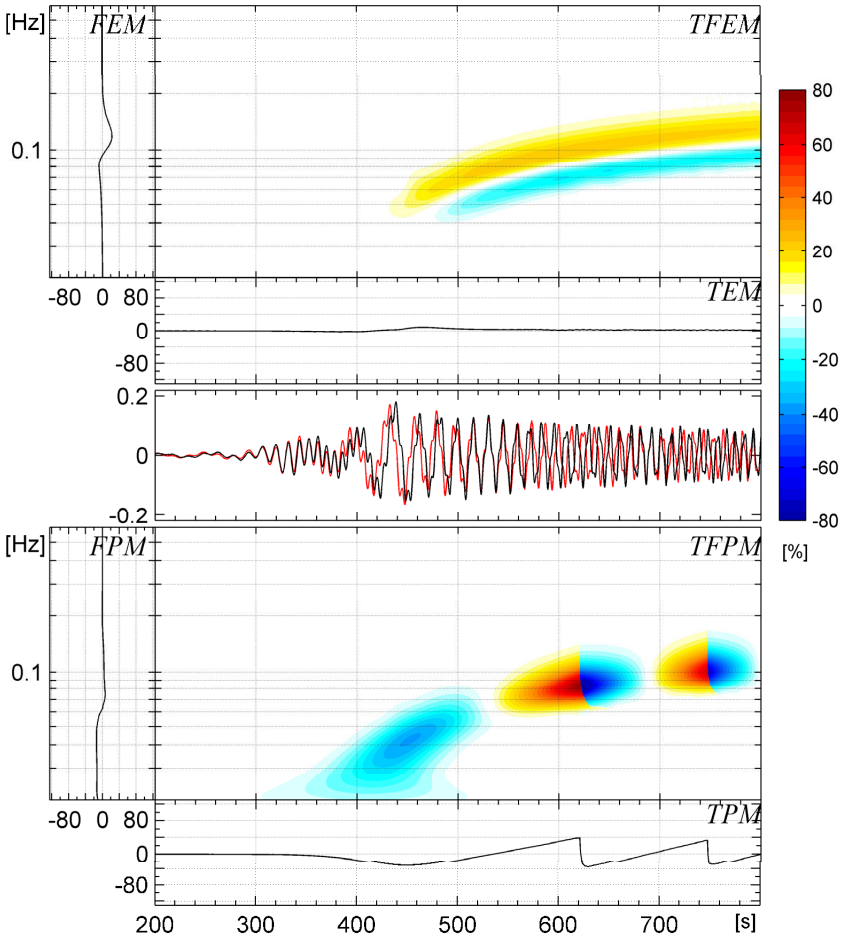

Figure 4. Globally normalized TF misfits between the composed dispersive signals $ur(1500, t)$, taken as reference, and $u(1500, t)$: TFEM and TFPM – TF envelope and phase misfits, TEM and TPM – time-dependent envelope and phase misfits, FEM and FPM – frequency-dependent envelope and phase misfits.

(f) show typical signatures of the differences between signals caused by frequency shift; compare with the simplest canonical situations in Kristekova *et al.* (2006). These typical signatures of the frequency shift include maxima with an alternating sign along the frequency axis in both the TF and frequency-dependent envelope misfits, and also significantly lower values of the time-dependent envelope misfit.

We can clearly recognize distinct features of the TF phase misfit $TFPM^{REF}_{GLOB}(t, f)$: a. The zero misfit (white colour) shows where $ur(t)$ and $u(t)$ are in phase. b. The positive misfits (warm colours) show where $u(t)$ is phase-advanced with respect to $ur(t)$. c. The negative misfits (cold colours) show where $u(t)$ is phase-delayed with respect to $ur(t)$. d. Lines of the discontinuous misfit-sign change (sudden colour change) delineate sudden (discontinuous) change of the phase difference between $ur(t)$ and $u(t)$ from π to $-\pi$, if we look in the positive direction along the time axis. Along the lines the signals are in antiphase. Note that whereas the phase difference between $ur(t)$ and $u(t)$ jumps from π to $-\pi$, the TF misfits values from both sides of the discontinuity may be smaller in absolute value than 100 per cent. There is no contradiction in this. This is just a simple consequence of the fact that the displayed misfits are globally normalized. Times of the occurrence of the phase jumps in the phase differences between the signals (when the signals are in antiphase) can be clearly identified also from the time-dependent phase misfit $TEM^{\mathrm{REF}}_{\mathrm{GLOB}}(t)$ as the times of a sudden change of the sign of the misfit values. Again, due to the global normalization, the $TPM^{\mathrm{REF}}_{\mathrm{GLOB}}(t)$ misfit values from both sides of the discontinuity may be smaller in absolute value than 100 per cent.

6.2 Recorded and numerically modelled earthquake motion

The observed three-component signal represents the ground motion recorded during a local small earthquake at the temporary seismic station in the Mygdonian basin near Thessaloniki, Greece. The computed three-component signal represents the numerically simulated motion for the preliminary structural model of the Mygdonian basin (Manakou *et al.* 2004). Both the recorded and computed signals are shown in Fig. 5. The relatively large differences between the observed and numerically simulated signals might mainly be due to the considerably simplified velocity model of the basin sediments. The observed signal is taken as a reference.

We present and discuss here locally and globally normalized TF representations of the signals, locally and globally normalized TF envelope and phase misfits, and locally and globally normalized TF envelope and phase goodness-of-fit criteria.

6.2.1 Locally normalized TF representations

The top panel of Fig. 6 shows three components of the recorded signal (red) and computed signal (black) together with their TF representations, that is $W^2(t, f)$. The TF representation of each

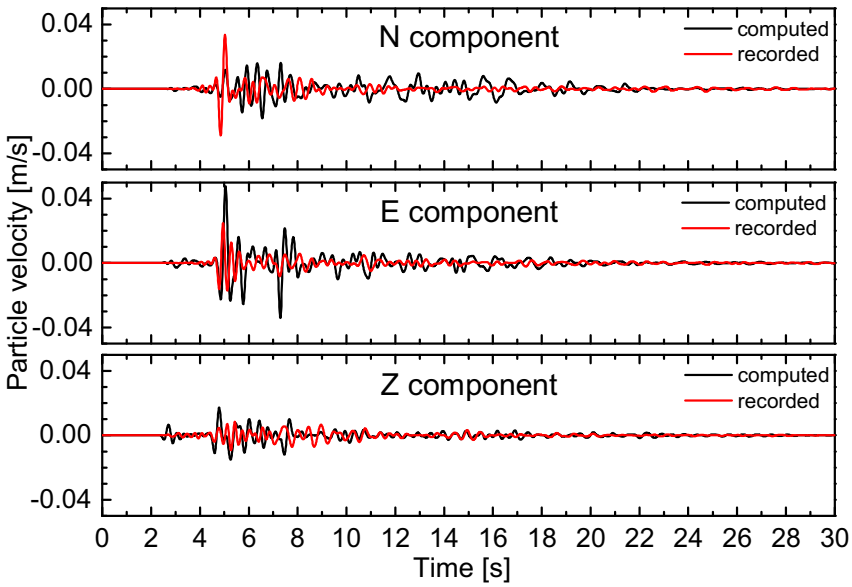

Figure 5. Recorded and computed three-component particle-velocity signals at the temporary seismic stations in the Mygdonian basin. N – north–south component, E – east–west component, Z – vertical component.

component is normalized with respect to the maximum $W^2(t, f)$ value for that component and then represented using the same logarithmic red-colour or grey scale covering the range of three orders of magnitude. The combination of the local normalization with the logarithmic scale enables us to see very well the detailed distribution of the signal energy larger than 0.1 per cent of the maximum. It is obvious that a direct visual comparison can neither quantify nor properly characterize differences between the TF representations of the signals.

6.2.2 *Globally normalized TF representations*

The top panel of Fig. 7 shows three components of the recorded signal (red) and computed signal (black) together with their TF representations, that is $W^2(t, f)$. The TF representation of each component is normalized with respect to the maximum $W^2(t, f)$ value from all three components; the same linear red-colour or grey scale is then applied to each normalized component. The combination of the global normalization with the linear scale shows very well the TF structure (pattern) of each component relative to the maximum $W^2(t, f)$ value, that is the energetically dominant TF contents of the signal. Although a bit easier than with the locally normalized TF representations, still a direct visual comparison provides neither quantification nor a proper characterization of the differences between the TF structures of the observed and computed signals.

6.2.3 *Locally normalized TF misfit criteria*

The middle panel of Fig. 6 displays the detailed anatomy of the TF envelope and phase misfits between corresponding components of the observed and computed signals in the entire considered TF range.

Due to relatively very large envelope-misfit values, all values above 200 per cent are shown in the same colour (magenta), that is, they are clipped at 200 per cent. Similarly, values below −200 per cent are shown using one colour (light green). Although the TF structure of the envelope misfits remains relatively complicated the TF envelope misfits show where the envelope of the computed signal is larger and where it is smaller compared to that of the observed signal. Because the misfits are locally normalized, they can attain very large values also at those (t, f) points or parts of the signal, where the envelope itself is relatively very small or negligible compared to the maximum envelope value (that is, where the energy of the signal is very small or negligible). It is just this feature of the locally normalized misfits that makes their interpretation relatively difficult. Therefore, when interpreting the misfits, one should always look also at the TF representations of the signals themselves.

The phase misfits show where the phase of the computed signal is advanced and where it is delayed compared to that of the observed signal. Note, however, that due to the complexity of the signals and nature of the phase misfit its TF structure is more complicated and consequently its interpretation more difficult than those of the envelope misfit.

6.2.4 *Globally normalized TF misfit criteria*

The globally normalized TF misfit criteria are shown in the middle panel of Fig. 7. The envelope/phase misfits clearly reflect those TF parts of the signals where the envelopes/phases differ and at least one of the signals is energetically significant. In other words, the globally normalized TF misfits account for both the envelope/phase difference at a (t, f) point and the significance of the envelope at that point with respect to the maximum envelope of the reference signal. Looking at the middle panel of Fig. 7 we can quite well 'sense' an overall level of disagreement between the compared signals.

6.2.5 *Locally normalized TF goodness-of-fit criteria*

The bottom panel of Fig. 6 shows the locally normalized TF envelope and phase goodness-of-fits. Although only four distinct colours were used and assigned to intervals of the goodness-of-fit values, the patterns of the TF envelope and phase goodness-of-fits are comparable with those of the clipped locally normalized TF misfits, that is, they are comparably complicated (note that not clipped misfits would be obviously even more complicated). This is due to the local normalization in both cases. It is clear that the local normalization

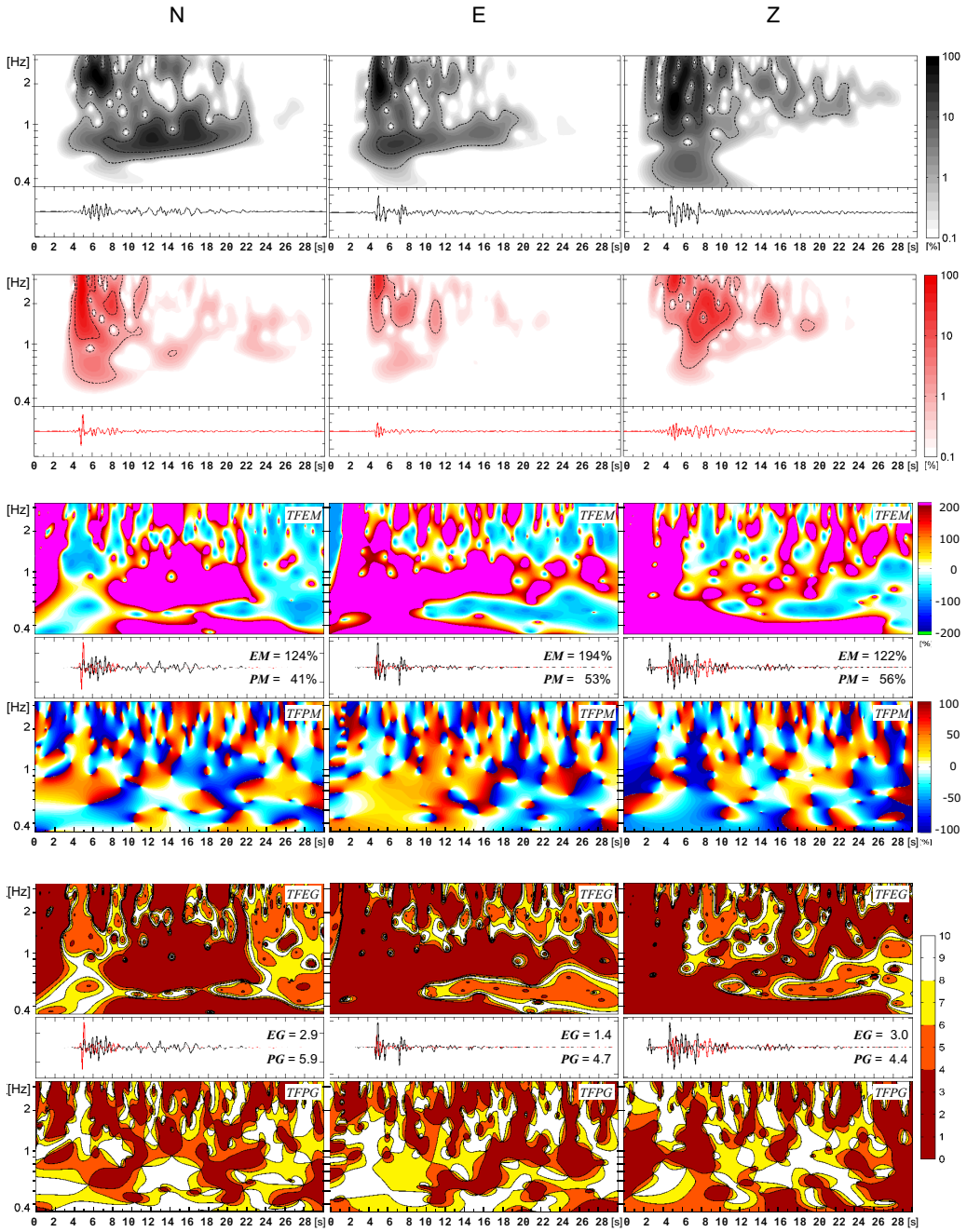

Figure 6. Top panel: three components of the recorded signal (red) and computed signal (black) together with their TF representations. The TF representation of each component is normalized with respect to the maximum W^2 (t, f) value for that component. Middle panel: Locally normalized TF envelope (*TFEM*) and phase (*TFPM*) misfits between corresponding components of the observed and computed signals. The envelope-misfit values above 200 per cent are shown in magenta, values below −200 per cent are shown in light green. Bottom panel: locally normalized TF envelope and phase goodness-of-fits.

makes the interpretation of the TF misfits and goodness-of-fits relatively difficult if the signals themselves are not simple. At the same time this relative complexity is unavoidable if the analysis requires seeing details of the difference, for example, related to specific part of the signals.

6.2.6 Globally normalized TF goodness-of-fit criteria

The bottom panel of Fig. 7 shows the globally normalized TF envelope and phase goodness-of-fits. Compared to all the preceding misfits and goodness-of-fits they provide the simplest and most robust tool for visualizing where in the TF plane the amplitudes and phases of the compared signals differ and where they do not. This is because they are goodness of fits, they are globally normalized, and they are displayed using distinct colours assigned to only four intervals of the goodness-of-fit values. Recall that the four colours represent, in fact, the simple verbal evaluation of the level of agreement given (as an example) in Fig. 1.

Based on the chosen globally normalized goodness-of-fits we can say that the level of the overall agreement in the *Z*-component is fair

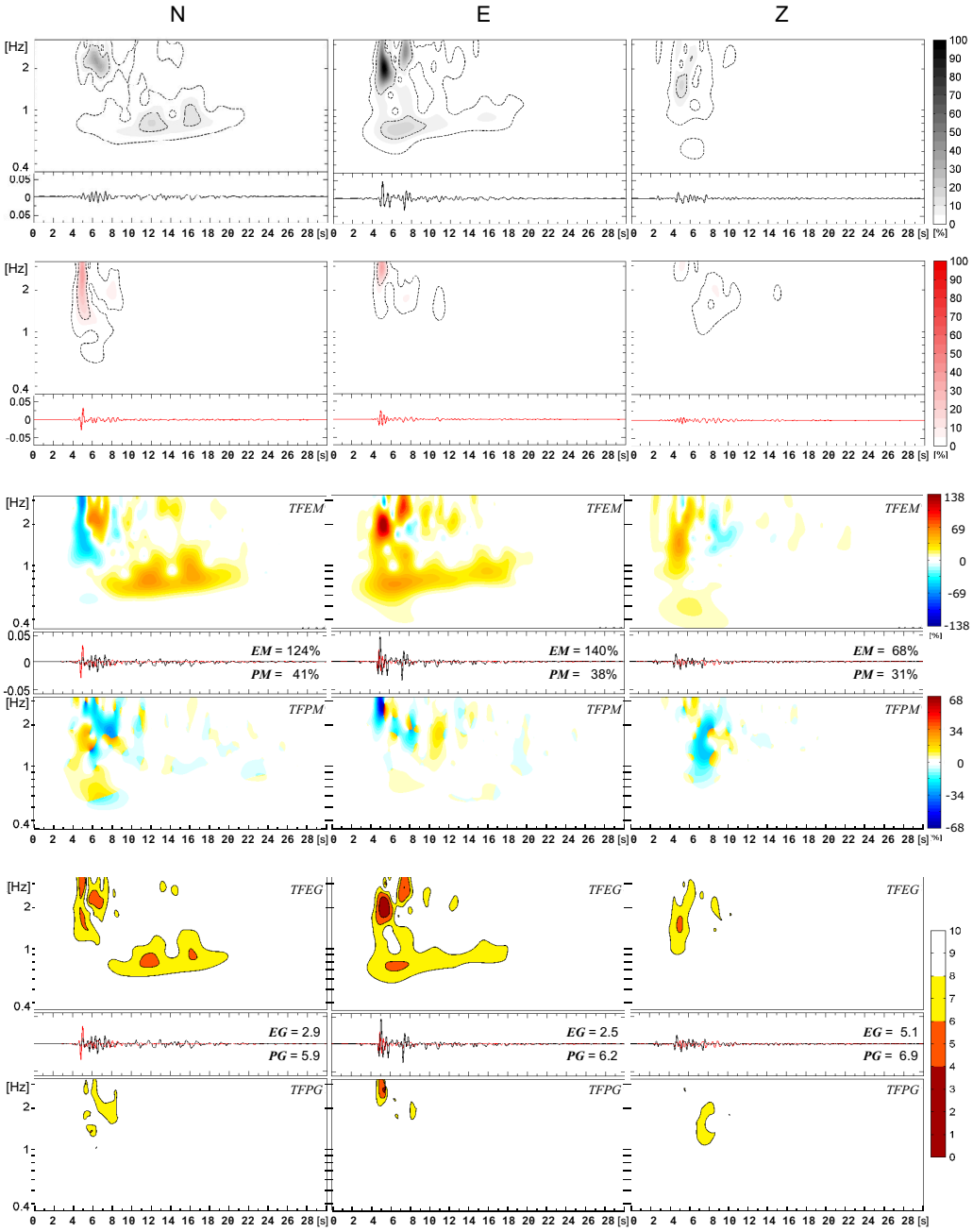

Figure 7. Top panel: Three components of the recorded signal (red) and computed signal (black) together with their TF representations. The TF representation of each component is normalized with respect to the maximum $W^2(t, f)$ value from all three components. Middle panel: Globally normalized TF envelope (*TFEM*) and phase (*TFPM*) misfits between corresponding components of the observed and computed signals. Bottom panel: Globally normalized TF envelope and phase goodness-of-fits.

in envelopes and good in phases. The level of the overall agreement in the horizontal components is poor in envelopes and fair-to-good in phases. The difference between the overall agreement in the *Z*-component and horizontal components is due to the presence of the wave group at lower frequencies and later times in the horizontal components, which is not present in the *Z*-component. The wave group is distinct in the numerically simulated motion. We can just note that its presence is likely due to the considerably simplified velocity structure of the basin sediments used in the computational model.

7 CONCLUSIONS

We presented a systematic extension and elaboration of the concept of the TF misfit criteria originally introduced by Kristekova *et al.* (2006), Kristekova *et al.* (2006) used the TF representation of signals

to define envelope and phase differences at a point of the TF plane, and the corresponding TF envelope and phase misfit criteria. They defined and numerically tested globally normalized criteria for one-component signals assuming that one of the compared signals can be considered a reference. The locally normalized criteria were defined but not tested and analysed.

The extension presented in this paper can be summarized as follows. We found more proper definition of the phase difference at a point of the TF plane. We defined TF misfit criteria for three-component signals. We distinguished two basic situations: 1. It is reasonable and possible to consider one of the compared signals a reference. 2. There is no reason, pertinent or attributable to the investigated problem, to choose one signal a reference. We also treated two principal normalizations of the misfits—local and global normalizations—in a unified way.

The values of the locally normalized misfit criteria for one (t, f) point depend only on the characteristics at that point. The locally normalized misfit criteria should be used if it is important to investigate the following.

(1) Relatively small parts of the signal (e.g. wave groups, pulses, transients, spikes, so-called seismic phases), no matter how large amplitudes of those parts are with respect to the maximum amplitude of the signal.
(2) A detailed TF anatomy of the disagreement between signals in the entire considered TF region.

The globally normalized misfit criteria give the largest weights to the local envelope/phase differences for those parts of the reference signal (true or formally algorithmically determined) in which the envelope reaches the largest values. The globally normalized misfit criteria should be used if it is reasonable

(1) to quantify an overall level of disagreement,
(2) to account for both the envelope/phase difference at a (t, f) point and the significance of the envelope at that point with respect to the maximum envelope of the reference signal, for example, in the earthquake ground motion analyses and earthquake engineering.

We also introduced the TF envelope and phase goodness-of-fit criteria derived from the TF misfit criteria. Thus the TF goodness-of-fit criteria are based on the complete signal representation and have the same TF structure as the TF misfits. They are suitable for comparing arbitrary time signals in their entire TF complexity.

The TF goodness-of-fit criteria quantify the level of agreement and are most suitable in the case of larger differences between the signals. They can be used when we look for the agreement rather than details of disagreement. The robust 'verbal quantification' enables us to see/find out the 'essential' level of agreement between the compared signals.

We numerically demonstrated the capability and important features of the TF misfit and goodness-of-fit criteria in two methodologically important examples.

Program package TF_MISFIT_GOF_CRITERIA (Kristekova *et al.* 2008a) is available at http://www.nuquake.eu/Computer_Codes/.

ACKNOWLEDGMENTS

The authors thank Jacobo Bielak and Martin Käser for their valuable reviews. This study was supported in part by the Scientific Grant Agency of the Ministry of Education of the Slovak Republic and the Slovak Academy of Sciences (VEGA) Project 1/4032/07 and the Slovak Research and Development Agency under the contract No. APVV-0435–07 (project OPTIMODE).

REFERENCES

Anderson, J.G., 2004. Quantitative measure of the goodness-of-fit of synthetic seismograms, in *13th World Conference on Earthquake Engineering Conference Proceedings,* Vancouver, Canada, Paper 243, on CD-ROM.

Benjemaa, M., Glinsky-Olivier, N., Cruz-Atienza, V.M., Virieux, J. & Piperno, S., 2007. Dynamic non-planar crack rupture by a finite volume method, *Geophys. J. Int.,* **171,** 271–285.

Bielak, J. *et al*. 2008. ShakeOut simulations: verification and comparisons, in *Proceedings 2008 SCEC Annual Meeting and Abstracts,* Vol. XVIII, SCEC, Palm Springs, CA, USA, p. 92.

Chaljub, E., Cornou, C. & Bard, P.-Y., 2009a. Numerical benchmark of 3D ground motion simulation in the valey of Grenoble, French Alps, Paper SB1, in *Proceedings of the Third International Symposium on the Effects of Surface Geology on Seismic Motion,* Grenoble, 30 August–1 September 2006, Vol. 2, 1365–1375 (LCPC editions).

Chaljub, E., Tsuno, S. & Bard, P.-Y., 2009b. Grenoble valley simulation benchmark: comparison of results and main learnings, Paper SB2, in *Proceedings of the Third International Symposium on the Effects of Surface Geology on Seismic Motio*n, Grenoble, 30 August–1 September 2006, Vol. 2, 1377–1436 (LCPC editions).

Daubechies, I., 1992. *Ten Lectures on Wavelets,* SIAM, Philadelphia.

Fichtner, A. & Igel, H., 2008. Efficient numerical surface wave propagation through the optimization of discrete crustal models—a technique based on non-linear dispersion curve matching (DCM), *Geophys. J. Int.,* **173,** 519–533.

Flandrin, P., 1999. *Time-Frequency / Time-Scale Analysis,* Academic Press, San Diego, CA, USA.

Gallovic, F., Barsch, R., de la Puente, J. & Igel, H., 2007. Digital library for computational seismology, *EOS,* **88,** 559.

Holschneider, M., 1995. *Wavelets: An Analysis Tool,* Clarendon Press, Oxford.

Igel, H., Barsch, R., Moczo, P., Vilotte, J.-P., Capdeville, Y. & Vye, E., 2005. The EU SPICE Project: a digital library with codes and training material in computational seismology, *Eos Trans. AGU,* **86,** Fall Meet. Suppl., Abstract S13A-0179.

Käser, M., Hermann, V. & de la Puente, J., 2008. Quantitative accuracy analysis of the discontinuous Galerkin method for seismic wave propagation, *Geophys. J. Int.,* **173,** 990–999.

Kristek, J. & Moczo, P., 2006. On the accuracy of the finite-difference schemes: the 1D elastic problem, *Bull. seism. Soc. Am.,* **96,** 2398–2414.

Kristek, J., Moczo, P. & Archuleta, R.J., 2002. Efficient methods to simulate planar free surface in the 3D 4th-order staggered-grid finite-difference schemes, *Stud. Geophys. Geod.,* **46,** 355–381.

Kristekova, M., 2006. Time-frequency analysis of seismic signals. *Dissertation thesis*. Geophysical Institute of the Slovak Academy of Sciences, Bratislava. (in Slovak)

Kristekova, M., Kristek, J., Moczo, P. & Day, S.M., 2006. Misfit criteria for quantitative comparison of seismograms, *Bull. seism. Soc. Am.,* **96,** 1836–1850.

Kristekova, M., Kristek, J. & Moczo, P., 2008a. The Fortran95 program package TF_MISFIT_and_GOF_CRITERIA and User's guide at http://www.nuquake.eu/Computer_Codes/

Kristekova, M., Moczo, P., Labak, P., Cipciar, A., Fojtikova, L., Madaras, J. & Kristek, J., 2008b. Time-frequency analysis of explosions in the ammunition factory in Novaky, Slovakia, *Bull. seism. Soc. Am.,* **98,** 2507–2516.

Manakou, M., Raptakis, D., Chávez-García, F., Makra, K., Apostolidis, P. & Pitilakis K., 2004. Construction of the 3D geological structure of Mygdonian basin (N. Greece), in *Proceedings of the 5th International Symposium on Eastern Mediterranean Geology,* Thessaloniki, Greece, 14–20 April 2004, Ref. S6-15.

Moczo, P., Ampuero, J.-P., Kristek, J., Day, S.M., Kristekova, M., Pazak, P., Galis, M. & Igel, H., 2006. Comparison of numerical methods for seismic wave propagation and source dynamics—the SPICE code validation, in *ESG 2006, Third International Symposium on the Effects of Surface*

Geology on Seismic Motion, Vol. 1, Grenoble, France, eds Bard, P.-Y. *et al.*, pp. 495–504 (LCPC editions).

Moczo, P., Kristek, J., Galis, M., Pazak, P. & Balazovjech, M., 2007. The finite-difference and finite-element modeling of seismic wave propagation and earthquake motion, *Acta Phys. Slovaca,* **57,** 177–406.

Pérez-Ruiz, J.A., Luzón, F. & García-Jerez, A., 2007. Scattering of elastic waves in cracked media using a finite-difference method, *Stud. Geophys. Geod.,* **51,** 59–88.

Qian, S., 2002. *Introduction to Time-Frequency and Wavelet Transforms,* Prentice Hall, NJ, USA.

Santoyo, M.A. & Luzón, F., 2008. Stress relations in three recent seismic series in the Murcia region, southeastern Spain, *Tectonophysics,* **457,** 86–95.

Tsuno, S., Chaljub, E., Cornou, C. & Bard, P.Y., 2006. Numerical benchmark of 3D ground motion simulation in the Alpine valley of Grenoble, France, *Eos Trans. AGU,* **87,** Fall Meet. Suppl., Abstract S41B-1335.